An Experimental and Theoretical Study of the Substituent Effects on the Redox Properties of 2-[(R-phenyl)amine]-1,4-naphthalenediones in Acetonitrile[||]

M. Aguilar-Martínez,*[,†] G. Cuevas,[‡] M. Jiménez-Estrada,[‡] I. González,[§] B. Lotina-Hennsen,[||] and N. Macías-Ruvalcaba[†]

Universidad Nacional Autónoma de México, Facultad de Química, Departamentos de Fisicoquímica y Bioquímica; Instituto de Química, 04510 México, D.F., México, and Universidad Autónoma Metropolitana−Iztapalapa, Departamento de Química, Apartado Postal 55−534, 09340 México D.F., México

Received February 1, 1999

We synthesized and analyzed 19 compounds of 3′- (*meta*-) and 4′- (*para*-) substituted 2-[(R-phenyl)-amine]-1,4-naphthalenediones (PANs) R = *p*-MeO, *p*-Me, *p*-Bu, *p*-Hex, *p*-Et, *m*-Me, *m*-Et, H, *p*-Cl, *p*-Br, *m*-F, *m*-Cl, *p*-$COCH_3$, *m*-CN, *m*-NO_2, *m*-COOH, and *p*-COOH. Despite the fact that the nitrogen atom, which binds the quinone with the *meta*- and *para*-substituted ring, interferes with the direct conjugation between both rings, the UV−vis spectra of these compounds show the existence of an intramolecular electronic transfer from the respective aniline to the *p*-naphthoquinone moiety. In accordance with this donor−acceptor character, the cyclic voltammograms of these compounds exhibit two, one-electron reduction waves corresponding to the formation of radical-anion and dianion, where the half-wave potential values vary linearly with the Hammett constants (σ_x). The analysis of the different voltammetric parameters (e.g., voltammetric function, anodic/cathodic peak currents ratio, and the separation between the anodic and cathodic potential peaks) show that with the exception of the carboxylic PAN derivatives, all compounds present the same reduction pathway. We investigated the molecular and electronic structures of these compounds using the semiempirical PM3 method and, within the framework of the Density Functional Theory, using the Becke 3LYP hybrid functional with a double ζ split valence basis set. Our theoretical calculations predict that, with the exception of the *p*-nitro compound, all the compounds are planar molecules where the conjugation degree of the nitrogen lone pair with the quinone system depends on the position and magnitude of the electronic effect of the substituent in the aniline ring. The Laplacians of the critical points ($\nabla^2\rho$), for the C−O bonds, show that the first reduction wave corresponds to the carbonyl group in α-position to the aniline, and that the second one-electron transfer is due to the C_4-O_2 carbonyl reduction. Thus, the higher reaction constant value (ρ) obtained for the second one-electron transfer is due to the fact that the displacement of the nonshared electrons of the amino nitrogen merely modifies the electron density of C_4-O_2 bond. The positive correlation between the LUMO energy values calculated for these compounds and the $E_{1/2}$ potentials corresponding to the C_1-O_1 carbonyl reduction show that the electron addition takes place at the lowest unoccupied molecular orbital, supporting the fact that this wave is also prone to the substituent effect.

Introduction

The quinone structure is found in many naturally occurring compounds and is associated with diverse biological activities.[1] Because of the inevitable exposure of humans to quinones and their inherent reactivity, many studies have focused on the chemistry and toxicology of these compounds.[2] In most cases, the biological activity of the quinones is related to their capacity to accept one or two electrons to form the corresponding radical-anion or dianion and to the acid−base properties of these species.[3] The ability of the quinones to accept one or two electrons depends directly on their chemical structures.[4] The electron-accepting capacity of these substances can be modified by directly adding a substituent to the quinone system[5] or by adding a substituted phenyl to the quinone ring.[6] For these types of compounds, the attracting or donor effects of the substituents are very important in affecting the redox properties of the quinone system, either facilitating or interfering with the charge transfer to the quinone. However, for some applications, gradual changes of these redox properties are required. To achieve such a gradual change, molecules of the type quinone-X-substituted phenyl have

* To whom correspondence should be addressed. Fax: (525) 6 16 22 17; e-mail: marthaa@servidor.unam.mx. Present address: Instituto de Química, Universidad Nacional Autónoma de México, 04510, México, D.F., México.

† Facultad de Química, Universidad Nacional Autónoma de México.

‡ Instituto de Química, Universidad Nacional Autónoma de México.

§ Universidad Autónoma Metropolitana−Iztapalapa.

|| Contribution no. 1691 of the Instituto de Quimíca, UNAM.

(1) Morton, R. A., Ed. *Biochemistry of Quinones*; Academic Press: New York, New York, 1965.

(2) Monks, T. J.; Hanzlik, R. P.; Cohen, G. M.; Ross, D.; Graham, D. G. *Toxicol. Appl. Pharmacol.* **1992**, *112*, 2−16.

(3) Wolstenholm, G. E. W.; O'Conner, C. M., Eds. *Quinones in Electron Transport*; Churchill: London, 1961.

(4) Zuman, P. *Substituents Effects in Organic Polarography*; Plenum Press: New York, New York, 1967.

(5) Huntington, J. L.; Davis, D. G. *J. Electrochem. Soc.* **1971**, *118* 57−62.

(6) Li, C. Y.; Caspar, M. L.; Dixon, D. W. *Electrochim. Acta* **1980**, *25*, 1135−1142. Qureshi, G. A.; Ireland, N. *Bull. Soc. Chim. Belg.* **1981**, *90*, 223−226.

10.1021/jo990186o CCC: $18.00
Published on Web 04/28/1999

Table 1. Structure of 2-[(R-Phenyl)amine]-1,4-naphthalenediones Synthesized in This Work

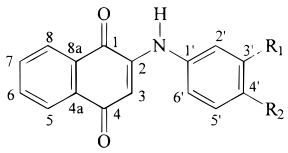

compound	R_1	R_2
PAN	H	H
p-MeOPAN	H	CH_3O
p-MePAN	H	CH_3
p-BuPAN[a]	H	n-C_4H_9
p-EtPAN[a]	H	C_2H_5
m-MePAN[a]	CH_3	H
m-EtPAN[a]	C_2H_5	H
p-HexPAN[a]	H	n-C_6H_{13}
p-ClPAN	H	Cl
p-BrPAN	H	Br
m-FPAN[a]	F	H
m-ClPAN	Cl	H
m-COOHPAN	COOH	H
p-COOHPAN	H	COOH
p-$COCH_3$PAN	H	$COCH_3$
p-CF_3PAN[a]	H	CF_3
m-CNPAN[a]	CN	H
m-NO_2PAN[a]	NO_2	H
p-NO_2PAN	H	NO_2

[a] These compounds have not been previously described, see Experimental Section.

been suggested,[7,8] with X being a heteroatom. The presence of the heteroatom allows modulation of the substituent's effect on the electronic properties of the quinone system, as well as modification of the geometry of the neutral molecules and of their reduction intermediates.[8]

1,4-Naphthoquinones, possessing an amine or a substituted amine group in the 2-position, have been the subject of study for many years due to their use in a variety of medical and biological applications such as antituberculars,[9] antimalarials,[10] antibacterials,[11] antitumor agents,[12] larvicides,[13] molluscicides,[13] herbicides,[14] and fungicides.[15] Our work reports on the synthesis and analysis of a series of 19 2-[(R-phenyl)amine]-1,4-naphthalenediones (Table 1), nine of which have not been previously described. These compounds were characterized by ^{1}H and ^{13}C NMR, IR, UV−visible spectroscopy, mass spectrometry, and cyclic voltammetry. To analyze the influence of the N-substituted phenyl group in quinone properties, we also studied the related quinone (naphthoquinone NQ). Through these analyses, we defined the influence of the donor and acceptor properties of the substituents on the electronic properties of the title compounds.

Through theoretical calculations using the semiempirical PM3 method and in the frame of the Density Functionals Theory (DFT), we performed the complete optimization of the geometry for some of the PANs studied experimentally. We also determined the Wiberg bond indexes, the natural charges, the densities at critical bond points, Laplacians, and ellipticities. Besides defining the spatial array of the neutral PAN molecules, these findings help clarify how the substituents in the aniline ring modify the electronic properties of the quinone system.

Since the biological activity of quinone compounds is related to the redox potentials of the quinone moiety, a systematic investigation of the substituent effects in PAN-like molecules could provide clues to the mechanisms of their biological activity. Such information will be useful for designing new molecules with greater and more specific biological activities.

Results and Discussion

Spectroscopic Results. PAN and its derivatives were insoluble in water. PANs containing electron-withdrawing substituents were found to be less soluble than the PANs with electron-releasing groups in both acetonitrile and ethanol. All the derivatives exhibited orange to dark-red colored solutions in ethanol. Dissolved compounds in EtOH had similar UV−vis spectra, with a band in the 240−272 nm region corresponding to the intense benzene and quinone $\pi-\pi^*$ electron transitions. We observed one band transfer at about 335 nm and a very broad, low-energy band in the visible region centered between 375 and 480 nm. We assume this second band is due to the $n-\pi^*$ transition of the carbonyl groups in the quinone. The *p*-NO_2PAN compound showed an additional, very intense band at 785 nm. Comparing the PAN spectrum with that of naphthoquinone (NQ), there is a significant shift in the λ_{max} absorption for the $n-\pi^*$ transition. This is an indication of the strong influence of the substituted aniline group at C_2 position of the naphthoquinone. The PAN derivatives show a similar electronic effect to that of PAN. The λ_{max} value, corresponding to the $n-\pi^*$ transition, was modified by the substituent in the aniline ring. We found that the electron donor groups (auxochromes) caused changes in the absorption of the $n-\pi^*$ transition at the longest wavelengths (batochromic effect), while the electron-accepting groups (chromophores) changed the absorption at shorter wavelengths (hipsochromic effect) (Table 2).

Plotting the $1/\lambda_{max}$ values obtained for each compound against the Hammett substituent constants σ_x, produced a linear correlation (eq 1).

$$1/\lambda_{max}\ (\mathrm{nm}^{-1}) = 1.43 \times 10^{-4}\sigma_x + 0.00214\ (n = 18,\ r = 0.9667) \quad (1)$$

This correlation indicates that even though the substituent is on the aniline group, the electronic properties of the quinone system are affected by the nature and position of the substituent. Theoretical studies explain this topic extensively. The σ_x constants used in this work are the standard Hammett values[16] and are included in Table 2.

(7) Stradins, J.; Glezer, V.; Turovska, B.; Markava, E.; Freimanis, J. *Electrochim. Acta* **1991**, *36*, 1219−1225. Glezer, V.; Turovska, B.; Stradins, J.; Freimanis, J. *Electrochim. Acta* **1990**, *35*, 1933−1940.
(8) Illescas, B.; Martin, N.; Segura, J. L.; Seoane, C.; Orti, E.; Viruela, P. M.; Viruela, R. *J. Org. Chem.* **1995**, *60*, 5643−5650.
(9) Oeriu, I.; Benesch, H. *Bull. Soc. Chim. Biol.* **1962**, *44*, 91−100. Oeriu, I. *Biokhimiya* **1963**, *28*, 380−383.
(10) Prescott, B. *J. Med. Chem.* **1969**, *12*, 181−182.
(11) Silver, R. F.; Holmes, H. L. *Can. J. Chem.* **1968**, *46*, 1859−1864.
(12) Hodnett, E. M.; Wongwiechintana, C.; Dunn, W. J.; Marrs, P. *J. Med. Chem.* **1983**, *26*, 570−574.
(13) Lopez, J. N. C.; Johnson, A. W.; Grove, J. F.; Bulhoes, M. S. *Cienc. Cult. (Sao Paulo)* **1977**, *29*, 1145−1149.
(14) U.S. Rubber Co., British Patent 862 489, 1959. Takeda Chemical Industry Co. Ltd, Japanese Patent 18 520, 1963. Ube Industries Ltd. Japanese Patent 126 725, 1979. Shell Internationale Research Maatschappij B. V., British Patent 1 314 881, 1973.
(15) Clark, N. G. *Pestic. Sci.* **1985**, *16*, 23−32.

Table 2. Electrochemical Parameters[a] and the Longest Wavelength Absorption Band[b] of 2-[(R-Phenyl)amine]-1,4-naphthalenediones (PANs)

			$i_{pc}v^{-1/2}c^{-1} \times 10^4$ (AV^{-1} $s^{1/2}$ mol^{-1} cm^3)		i_{pa}/i_{pc}		ΔE_p (mV)		$E_{1/2}$ (mV)	
compound	σ_x[c]	λ_{max} (nm)	wave I	wave II	wave I	wave II	wave I	wave II	wave I	wave II
NQ		[d]	0.79	0.69	1.01	1.11	73	73	−1036	−1495
p-MeOPAN	−0.27	480.0	0.75	0.72	1.00	0.89	69	74	−1236	−1809
p-MePAN	−0.17	473.1	0.81	0.74	0.99	0.76	67	124	−1216	−1773
p-BuPAN	−0.16	472.9	0.81	0.70	0.95	0.71	64	86	−1217	−1770
p-HexPAN	−0.16[e]	474.6	0.76	0.63	1.05	0.72	70	68	−1215	−1720
p-EtPAN	−0.15	472.4	0.75	0.71	1.02	0.83	64	70	−1218	−1749
m-MePAN	−0.07	468.3	0.69	0.62	0.98	0.76	73	81	−1213	−1685
m-EtPAN	−0.07	469.1	0.72	0.64	0.92	0.94	75	80	−1216	−1665
PAN	**0.0**	**465.5**	**0.77**	**0.67**	**0.99**	**0.90**	**70**	**69**	**−1209**	**−1685**
p-ClPAN	0.23	460.9	0.66	0.71	1.08	0.62	65	65	−1173	−1608
p-BrPAN	0.23	463.4	0.70	0.68	1.01	0.78	61	59	−1176	−1642
m-FPAN	0.34	456.4	0.75	0.70	1.06	0.92	70	82	−1163	−1567
m-ClPAN	0.37	456.8	0.76	0.67	1.00	0.93	70	64	−1145	−1520
p-$COCH_3$PAN	0.50	459.1	0.77	0.72	0.98	0.96	68	66	−1126	−1554
p-CF_3PAN	0.54	452.0	0.66	0.63	0.93	0.97	70	63	−1147	−1602
m-CNPAN	0.56	448.0	0.82	0.68	1.08	0.84	97	74	−1133	−1612
m-NO_2PAN	0.71	444.4	[f]	[f]	[f]	[f]	115	39	−1104	−1312
p-NO_2PAN	0.78	443.1	[f]	[f]	[f]	[f]	108	[f]	−1067	[f]
m-COOHPAN	0.37	459.5	[f]	[f]	0.29	0.90	162	64	−880	−1211
p-COOHPAN	0.45	459.5	[f]	[f]	0.14	[f]	341	[f]	−917	[f]

[a] Measured by cyclic voltammetry (mV vs Fc/Fc^+), 0.1 M Et_4NBF_4/acetonitrile with Pt electrode (3.14 mm^2). [b] In ethanol, corresponding to the n−π^* transition of the quinone carbonyl group. [c] The standard Hammett values were taken from ref 16. [d] Not observed. [e] Determined value in this work. [f] Because the waves were ill-defined, these values could not be accurately determined.

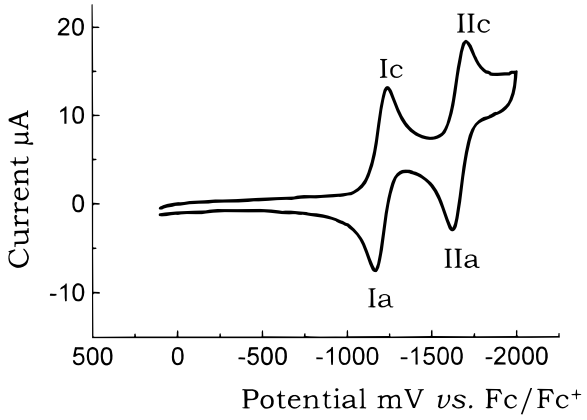

Figure 1. Typical cyclic voltammogram of 1 mM PAN in 0.1 M Et_4NBF_4/acetonitrile obtained in Pt electrode (3.14 mm^2), scan rate 100 mV/s. The cathodic (c) and anodic (a) peaks are indicated in the figure.

Electrochemical Results. The redox potentials of the PAN compounds determined in this work were measured by cyclic voltammetry at room temperature using a platinum electrode in acetonitrile solvent and 0.1 M tetraethylamonium tetrafluoroborate as the supporting electrolyte. The voltammograms were recorded in the potential range from 0.0 to −2.4V vs Fc/Fc^+. Figure 1 shows the typical electrochemical behavior of PAN, which proceeded in two one-electron diffusion stages, PAN + e ⇌ $PAN^{\bullet -}$ and $PAN^{\bullet -}$ + e ⇌ PAN^{2-}. The same behavior was observed within the sweep range of 50 to 1000 mV s^{-1}. At scan rates higher than 1000 mVs^{-1}, however, small distortions were detected in the cyclic voltammograms that made determination of the corresponding electrochemical parameters difficult. For this reason, in our discussion of the results only the data obtained between 50 and 1000 mVs^{-1} were considered. The half-wave potential values $E_{1/2}$ for both waves were evaluated from the voltammograms obtained at a sweep rate of 100 mVs^{-1}, as $E_{1/2} = (E_{pa}+E_{pc})/2$, where E_{pa} and E_{pc} correspond to anodic and cathodic peak potentials, respectively, for each wave.

With the exception of the *m*-COOHPAN, *p*-COOHPAN, *m*-NO_2PAN, and *p*-NO_2PAN compounds, which presented more complex cyclic voltammograms, the electrochemical behavior for all the other PAN derivatives and also for NQ was similar to that shown in Figure 1. In all PANs, the cathodic peak current (i_{pc}) vs the square root of the sweep rate ($v^{1/2}$), produced a linear relationship with zero intercept for both peaks, indicating the lack of detectable chemical kinetic complications.[17] This behavior was confirmed by consistency of the voltammetric function ($i_{pc}v^{-1/2}c^{-1}$) with the sweep rate. Due to the different solubilities of the PANs in acetonitrile, the concentration used for the voltammetric studies varied. Voltammetric function values were standardized for concentration and reported as $i_{pc}v^{-1/2}c^{-1}$, where i_{pc} represents the cathodic peak current of the first or second reduction peak, v is the scan rate, and c is the concentration of compound in mol/cm^3.

Table 2 shows that the values of the current function, $i_{pc}v^{-1/2}c^{-1}$, for both waves are approximately the same. This indicates the one-electron transfer for each wave and that the diffusion coefficients are approximately equal for the compounds analyzed. Such a result is to be expected since the molecules are quite similar in size and shape. Furthermore, the reversibility degree is indicated by the relationship i_{pa}/i_{pc}, which is close to one in value as described for reversible systems. The values of ΔEp ($E_{pa} - E_{pc}$) also approach the theoretical value of 60 mV reported for one-electron reversible systems.[18] The $E_{1/2}$ values (Table 2) for the first one-electron transfer, corresponding to the formation of the radical-anions, are in the potential range of −1036 to −1236 mV. For the

(16) Hansch, C.; Leo, A.; Taft, R. W. *Chem. Rev.* **1991**, *91*, 165−195.

(17) Bard, A. J.; Faulkner, L. R. *Electrochemical Methods. Fundamentals and Aplications*; John Wiley & Sons: New York, 1980.

(18) Heinze, J. *Angew. Chem., Int. Ed. Engl.* **1984**, *23*, 831−847.

second one-electron transfer, the $E_{1/2}$ values, leading to the formation of the corresponding dianions, fall within the range of −1312 to −1809 mV.

The differences in voltammetric behavior observed for the *m*-COOHPAN and *p*-COOHPAN compounds as compared to the other PANs indicate that for these compounds there must be an additional effect on the electrode process. Since carboxylic acids tend to liberate a hydrogen ion easily, the autoprotonation reaction of the different species in solution can actually take place. [19]

The complexity of the cyclic voltammograms observed for *m*-NO_2PAN and *p*-NO_2PAN indicates that the nitro group is also electroactive in the cathodic zone studied. The reduction potentials for the nitro and the quinone groups unfortunately are similar enough so that differentiation of the independent stages from the overall reduction process is difficult. Because of this we were unable to assess all the voltammetric parameters for these derivatives.

Based on the similarities in the voltammetric measurements (Table 2), we can presume that all these quinones are reduced by the same mechanism.[4] So being, one would expect to find consistency among these substances for other molecular properties such as substituent electronic effects (Hammett substituent constant σ_x), spectroscopic parameters, and molecular-orbital calculations.

Substitution Effects. The introduction of the 3′- (*meta*-) and 4′- (*para*-) substituted anilines on the 2-position of 1,4-naphthoquinone (NQ), produces a considerable cathodic shift for the two, one-electron steps (Table 2). Even though the substituent is not directly conjugated with the quinone group, the substitution effect of the aniline system on the electrochemical reduction of the naphthoquinones was evident. The electron-attracting groups (fluoro, chloro, bromo, cyano, nitro, acetyl, and trifluoromethyl) displaced the $E_{1/2}$ of PAN to less negative values. The electron-donor groups (methoxy, methyl, ethyl, butyl, and hexyl) made the reduction of quinone more difficult than that of PAN.

The four alkyl side chains in the compounds *m*-MePAN, *p*-MePAN, *m*-EtPAN, *p*-EtPAN, *p*-BuPAN, and *p*-HexPAN proved to be similar electron-donors since the magnitude of the observed cathodic shift with respect to that of PAN for the first wave was roughly equal. The values for each were as follows: *p*-methyl, 7 mV; *p*-ethyl, 9 mV; *m*-methyl, 4 mV; *m*-ethyl, 8 mV; *p*-butyl, 8 mV; *p*-hexyl, 6 mV. The methoxy group, as expected, was consistently a more powerful electron-donor than the alkyl groups, as it exerted a cathodic shift of 27 mV, a value approximately four times that recorded for the alkyl groups.

The chloro and bromo substituents in *para*-positions exerted approximately equal anodic shifts (*p*-chloro, 36 mV and *p*-bromo, 33 mV). However, the anodic shift was greater with halogens in *meta*-positions (*m*-FPAN, 46 mV and *m*-ClPAN, 64 mV). This confirmed that the inductive effect of the halogen groups at this position is much more pronounced than their resonance effect.[16]

Substituents such as cyano, acetyl, and nitro, which are strongly unsaturated at the point of attachment with the aniline ring, proved to be more powerful electron-acceptors than the trifluoromethyl and halogens. The magnitudes of the observed anodic shifts for these compounds, with respect to PAN (*p*-$COCH_3$PAN, 83 mV; *m*-CNPAN, 76 mV; *m*-NO_2PAN, 105 mV; *p*-NO_2PAN, 142 mV) were larger than those for *p*-CF_3PAN (62 mV) and for halogens. The nitro group in *meta*-position was found to be a weaker electron-accepting group than the same group in *para*-position, indicating that in this case the resonance effect is more pronounced that the inductive, even when there is not a direct electron displacement in these compounds.

The electron density, as induced by their substituents and measured as a function of $E_{1/2}$ for wave I, increases in the following order: *p*-NO_2 < *m*-NO_2 < *p*-COMe < *m*-CN < *m*-Cl < *p*-CF_3 < *m*-F < *p*-Cl < *p*-Br < H < *m*-Me < *p*-Hex < *p*-Me < *p*-Bu, *m*-Et < *p*-Et < *p*-MeO.

To establish a quantitative measure of the substituent effect over the electrochemical reduction of the unsubstituted PAN system, the $\Delta E_{1/2}$ potentials were correlated with the σ_x Hammett constants, where $\Delta E_{1/2}$ is the difference in half-wave potentials between the substituted quinone and the parent reference compound, PAN. The $\Delta E_{1/2}$ for the transformation of Q to $Q^{\bullet -}$ varies linearly with σ_x Equation 2 represents the linear regression obtained.

$$\Delta E_{1/2}(\text{mV}) = 139\ \sigma_x + 3.71\ (n = 16,\ r = 0.9771) \quad (2)$$

In the regression analysis, the compounds *m*-COOHPAN and *p*-COOHPAN were far outside the trend of a linear relationship shown by the other compounds in the series and so were not considered for the linear regression treatment. The results confirm that these compounds undergo a different reduction mechanism,[4] which, as mentioned above, is due to an autoprotonation process. The good correlation between the electroreduction potentials for the first one-electron reversible stage with the Hammett's σ_x constants for all the other PANs substantiates that the electrochemical reduction mechanism is the same for all of them.

In the Hammett−Zuman context, the slope of eq 2, 139 mV, corresponds to the reaction constant, ρ_{π}, which is characteristic of a given reaction and denotes the sensitivity of the reaction to the electronic effects of the various substituent groups studied. The positive value of ρ_{π} implies that the reaction is facilitated by a low electron density on the electroactive group, and indicates that the electron-accepting ability of these PAN derivatives bears a linear relationship to the substituents electronic perturbation. From PAN and *p*-HexPAN $E_{1/2}$ potentials obtained for wave I (Table 2) and using eq 2, we estimated the σ_p Hammett value for the hexyl substituent ($\sigma_p = -0.16$), which had not been previously reported. The σ_p value obtained for the hexyl group substituted in the *para*-position is very close to the σ_p values reported for similar alkyl groups.[16]

To establish the influence of the substituent on the radical-anion ($Q^{\bullet -}$) formed during the first reduction of the PAN derivatives, the variation of $\Delta E_{1/2}$ of the second reduction peak is presented as a function of σ_x. To assess correctly the effect of the substituents in this type of reaction, $\sigma_{x}^{\bullet -}$ constants for radical-anions should be used. Since the $\sigma_{x}^{\bullet -}$ values for the compounds we studied are not available, we used the σ_x values as an approximation

(19) González, F.; Aceves, J. M.; Miranda, R.; González, I. *J. Electroanal. Chem.* **1991**, *310*, 293−303. Ortiz, J. L., Delgado, J., Baeza, A., González, I., Sanabria, R.; Miranda, R. *J. Electroanal. Chem.* **1996**, *411*, 103−107.

Table 3. Geometry of NQ, *p*-NO_2PAN, *p*-CNPAN, *p*-FPAN, PAN, *p*-MePAN, *p*-MeOPAN with the PM3 Method

bond	NQ	NO_2	CN	F	H	Me	MeO
C_1-O_1	1.219	1.218	1.220	1.220	1.220	1.220	1.221
C_1-C_2	1.486	1.506	1.513	1.513	1.513	1.513	1.513
C_2-C_3	1.334	1.347	1.352	1.353	1.353	1.354	1.354
C_3-C_4		1.481	1.473	1.471	1.470	1.470	1.469
C_4-O_2		1.218	1.221	1.222	1.222	1.222	1.222
C_4-C_{4a}	1.489	1.488	1.489	1.489	1.490	1.490	1.490
$C_{4a}-C_5$	1.395	1.393	1.394	1.394	1.395	1.395	1.395
C_5-C_6	1.393	1.393	1.392	1.392	1.392	1.392	1.392
C_6-C_7	1.388	1.389	1.389	1.389	1.389	1.389	1.389
C_7-C_8		1.393	1.392	1.392	1.392	1.392	1.391
C_8-C_{8a}		1.395	1.396	1.397	1.397	1.397	1.397
$C_{4a}-C_{8a}$	1.405	1.403	1.402	1.402	1.402	1.402	1.402
C_2-N		1.433	1.408	1.405	1.403	1.403	1.401
$N-H$		0.998	0.999	0.999	0.999	0.999	0.999
$N-C_{1'}$		1.428	1.422	1.472	1.428	1.429	1.431
$C_{1'}-C_{2'}$		1.409	1.414	1.412	1.414	1.411	1.409
$C_{2'}-C_{3'}$		1.384	1.383	1.383	1.389	1.385	1.386
$C_{3'}-C_{4'}$		1.401	1.400	1.402	1.395	1.397	1.399
$C_{4'}-R$		1.493	1.423	1.343	1.095	1.485	1.381
$C_{1'}-C_{6'}$		1.402	1.400	1.399	1.398	1.398	1.400
$C_{6'}-C_{5'}$		1.386	1.399	1.390	1.392	1.390	1.388
$C_{5'}-C_{4'}$		1.400	1.394	1.397	1.388	1.393	1.401
$O_1-C_1-C_2$	120.4	121.2	120.5	120.6	120.6	120.7	120.6
$C_1-C_2-C_3$	122.3	120.2	119.8	119.7	119.7	119.7	119.6
C_1-C_2-N		117.1	114.1	114.2	114.3	114.3	114.3
C_2-N-H		112.5	114.6	114.7	114.8	114.8	114.8
$C_2-N-C_{1'}$		123.5	132.6	132.6	132.6	132.6	132.7
$C_2-C_3-C_4$	122.3	120.2	123.3	123.4	123.5	123.4	119.6
$H-N-C_{1'}$		11.7	112.8	112.6	112.6	112.6	112.5
$C_{1'}-C_{2'}-C_{3'}$		120.5	120.9	121.0	120.5	120.7	121.2
$C_{1'}-C_{6'}-C_{5'}$		120.5	120.5	120.6	120.1	120.2	120.6
$C_{8a}-C_1-C_2$		116.5	117.9	117.9	117.9	117.9	117.9
$C_2-N-C_{1'}$-$C_{2'}$		153.4	180.0	180.0	180.0	180.0	180.0
$O_1-C_1-C_2-N$	0.0	11.4	0.0	0.0	0.0	0.0	0.0
$H-N-C_2-C_1$		8.6	0.0	0.0	0.0	0.0	0.0
$C_1-C_2-C_3-C_4$	0.0	1.8	0.0	0.0	0.0	0.0	0.0
$C_2-C_3-C_4-C_{4a}$	0.0	14.7	0.0	0.0	0.0	0.0	0.0
$C_2-C_1-C_{8a}-C_8$	180.0	163.8	180.0	180.0	180.0	180.0	180.0
$C_{8a}-C_1-C_2-N$	180.0	168.2	180.0	180.0	180.0	180.0	180.0
$C_1-C_2-N-C_{1'}$		130.3	180.0	180.0	180.0	180.0	180.0
$O_1-C_2-C_4-O_2$	0.0	2.4	0.0	0.0	0.0	0.0	0.0
$O_1-H(N)$		2.377	2.274	2.277	2.280	2.282	2.280

of the substituent effect, as suggested by Hammett.[20] The $\Delta E_{1/2}$ from the reduction of $Q^{\bullet-}$ to Q^{2-} also showed an acceptable linear relationship with the Hammett constants (eq 3).

$$\Delta E_{1/2} = 319\sigma_x - 0.27\,(n = 15,\ r = 0.8536) \quad (3)$$

The value of the slope is higher than the one obtained for the $Q/Q^{\bullet-}$ reduction, indicating that the radical-anions are more intensely affected by the substituents than the corresponding PANs. This will be discussed in detail in the theoretical section, below.

For the *m*-COOHPAN, *p*-COOHPAN compounds, where it was impossible to include the $\Delta E_{1/2}$ values in the relationship of 2 and 3 because of their complex electrochemical behavior, the ($1/\lambda_{max}$ vs σ_x) relationship for these compounds (eq 1) establishes that the substituent effect shows the same behavior as for the other PANs.

Theoretical Calculations. To understand the experimental observations reported above, we performed the complete geometrical optimization of *p*-MeOPAN, *p*-MePAN, PAN, *p*-FPAN, *p*-CF_3PAN, *p*-CNPAN, *p*-NO_2-PAN, and the naphthoquinone (NQ) (Tables 3 and 4) using the semiempirical PM3 method within the framework of the Density Functional Theory[21] with the Becke3LYP hybrid functional, by using a double ζ split valence basis set. The relevant geometric data are included in Tables 3 and 4. Tables 5 and 6 show the natural charges and the Wiberg bond indexes, calculated with the NBO program[22] at Becke3LYP/6-31G(*d*,*p*) level, as well as the densities of the relevant critical points,

(20) Hammett, L. P. *Physical Organic Chemistry*; McGraw-Hill: New York, 1940.

Table 4. Geometry of NQ, *p*-NO_2PAN, *p*-CNPAN, *p*-FPAN, *p*-CF_3PAN, PAN, *p*-MePAN, *p*-MeOPAN at Becke3LYP/6-31G(*d*,*p*) Level

bond	NQ	NO_2	CN	CF_3	F	H	Me	OMe
C_1-O_1	1.226	1.228	1.229	1.229	1.229	1.229	1.229	1.229
C_1-C_2	1.485	1.513	1.517	1.517	1.517	1.517	1.516	1.516
C_2-C_3	1.343	1.363	1.364	1.365	1.368	1.368	1.368	1.370
C_3-C_4		1.462	1.461	1.459	1.456	1.456	1.455	1.454
C_4-O_2		1.229	1.230	1.231	1.232	1.232	1.233	1.233
C_4-C_{4a}	1.429	1.498	1.497	1.497	1.499	1.499	1.499	1.499
$C_{4a}-C_5$	1.398	1.395	1.395	1.395	1.395	1.395	1.395	1.395
C_5-C_6	1.393	1.395	1.395	1.395	1.395	1.395	1.395	1.395
C_6-C_7	1.399	1.399	1.399	1.399	1.399	1.399	1.399	1.399
C_7-C_8		1.393	1.392	1.392	1.392	1.392	1.392	1.392
C_8-C_{8a}		1.400	1.401	1.401	1.401	1.401	1.401	1.401
$C_{4a}-C_{8a}$	1.409	1.407	1.406	1.406	1.406	1.406	1.406	1.406
C_2-N		1.369	1.368	1.367	1.362	1.362	1.361	1.360
$N-H$		1.018	1.020	1.019	1.019	1.019	1.018	1.018
$N-C_{1'}$		1.392	1.391	1.395	1.400	1.400	1.400	1.402
$C_{1'}-C_{2'}$		1.411	1.412	1.409	1.410	1.409	1.407	1.405
$C_{2'}-C_{3'}$		1.385	1.383	1.387	1.388	1.389	1.398	1.391
$C_{3'}-C_{4'}$		1.396	1.407	1.397	1.391	1.397	1.401	1.400
$C_{4'}-R$		1.463	1.431	1.502	1.349	1.085	1.510	1.365
$C_{1'}-C_{6'}$		1.408	1.407	1.406	1.404	1.404	1.404	1.407
$C_{6'}-C_{5'}$		1.389	1.390	1.391	1.395	1.396	1.393	1.389
$C_{5'}-C_{4'}$		1.393	1.403	1.396	1.387	1.393	1.400	1.400
$O_1-C_1-C_2$	120.5	118.9	118.9	119.0	119.1	119.1	119.1	119.2
$C_1-C_2-C_3$	122.2	120.5	119.9	119.8	119.8	119.7	119.8	119.8
C_1-C_2-N		110.6	109.8	109.8	109.9	109.9	110.0	110.0
C_2-N-H		111.1	109.8	109.9	110.0	110.1	110.1	110.1
$C_2-N-C_{1'}$		132.0	134.8	134.9	134.7	134.8	134.8	134.8
$C_2-C_3-C_4$	122.2	120.5	122.6	122.7	122.7	122.8	122.8	119.8
$H-N-C_{1'}$		116.9	115.4	115.3	115.3	115.1	115.1	115.1
$C_{1'}-C_{2'}-C_{3'}$		120.8	121.2	121.0	121.3	120.9	121.0	121.7
$C_{1'}-C_{6'}-C_{5'}$		120.1	120.2	120.0	120.3	119.9	120.0	120.4
$C_{8a}-C_1-C_2$		118.2	118.5	118.5	118.5	118.5	118.5	118.4
$C_2-N-C_{1'}-C_{2'}$		159.9	180.0	180.0	180.0	180.0	180.0	180.0
$O_1-C_1-C_2-N$	0.0	1.46	0.0	0.0	0.0	0.0	0.0	0.0
$H-N-C_2-C1$		6.3	0.0	0.0	0.0	0.0	0.0	0.0
$C_1-C_2-C_3-C_4$	0.0	2.6	0.0	0.0	0.0	0.0	0.0	0.0
$C_2-C_3-C_4-C_{4a}$	0.0	0.0	0.0	0.0	0.0	0.0	0.0	0.0
$C_2-C_1-C_{8a}-C_8$	180.0	178.1	180.0	180.0	180.0	180.0	180.0	180.0
$C_{8a}-C_1-C_2-N$	180.0	178.8	180.0	180.0	180.0	180.0	180.0	180.0
$C_1-C_2-N-C_{1'}$		173.7	180.0	180.0	180.0	180.0	180.0	180.0
$O_1-C_2-C_4-O_2$	0.0	62.2	180.0	180.0	180.0	180.0	180.0	0.0
$O_1-H(N)$		2.034	1.983	1.985	1.993	1.997	1.997	1.995
$H_3-H_{6'}$		2.027	1.827	1.832	1.824	1.827	1.827	1.831

Table 5. Natural Charges at Becke3LYP/6-31G(*d*,*p*) Level

R_2	NQ	NO_2	CN	CF_3	F	H	Me	MeO
C_1	0.51	0.54	0.54	0.54	0.54	0.54	0.54	0.54
C_2	−0.25	0.15	0.15	0.15	0.15	0.15	0.15	0.15
C_3		−0.35	−0.34	−0.35	−0.36	−0.36	−0.36	−0.37
C_4		0.50	0.50	0.50	0.50	0.50	0.50	0.50
C_{4a}	−0.12	−0.09	−0.09	−0.09	−0.09	0.09	−0.08	−0.09
C_5	−0.19	−0.19	−0.19	−0.19	−0.19	−0.20	−0.20	−0.20
C_6	−0.22	−0.21	−0.21	−0.21	−0.21	−0.21	−0.21	−0.21
C_7		−0.23	−0.23	−0.23	−0.23	−0.23	−0.23	−0.23
C_8		−0.18	−0.18	−0.18	−0.18	−0.18	−0.18	−0.18
C_{8a}		−0.13	−0.13	−0.13	−0.13	−0.13	−0.13	−0.13
O_1		−0.55	−0.55	−0.55	−0.55	−0.55	−0.56	−0.56
O_2		−0.53	−0.54	−0.54	−0.55	−0.55	−0.55	−0.55
N		−0.57	−0.57	−0.57	−0.56	−0.56	−0.56	−0.56
$C_{1'}$		0.19	0.18	0.18	0.15	0.16	0.15	0.14
$C_{2'}$	−0.51	−0.26	−0.26	−0.25	−0.25	−0.26	−0.25	−0.24
$C_{3'}$		−0.20	−0.18	−0.20	−0.29	−0.22	−0.22	−0.31
$C_{4'}$		0.04	−0.19	−0.19	0.41	−0.25	−0.04	0.31
$C_{6'}$		−0.27	−0.26	−0.26	−0.25	−0.26	−0.26	−0.25
$C_{5'}$		−0.19	−0.17	−0.24	−0.29	−0.22	−0.21	−0.26

Table 6. Wiberg Bond Indexes (WBI), and Properties of the Relevant Bond Critical Points, in the Electronic Density of the Referred Quinones at Becke3LYP/6-31G(*d*,*p*) Level

R_2	enlace	WBI	ρ	$\nabla^2(\rho)$	ϵ
NQ	C_1-C_2	1.05	0.157	−0.100	0.240
	C_2-C_3	1.08	0.163	0.084	1.082
	O_1-C_1	1.74	0.259	0.064	0.471
MeO	C_1-C_2	1.0	0.261	−0.632	0.099
	C_2-C_3	1.54	0.324	−0.905	0.310
	C_3-C_4	1.14	0.286	−0.741	0.155
	O_1-C_1	1.71	0.394	0.168	0.029
	O_2-C_4	1.67	0.393	0.078	0.054
	C_2-N	1.20	0.317	−0.855	0.096
	$N-C_{1'}$	1.06	0.290	−0.816	0.095
	O−H		0.028	0.100	0.231
	H−H		0.015	0.052	0.104
Me	C_1-C_2	1.0	0.261	−0.638	0.098
	C_2-C_3	1.55	0.324	−0.910	0.311
	C_3-C_4	1.13	0.286	−0.739	0.152
	O_1-C_1	1.71	0.395	0.171	0.030
	O_2-C_4	1.66	0.393	0.084	0.054
	C_2-N	1.19	0.317	−0.868	0.092
	$N-C_{1'}$	1.07	0.290	−0.820	0.078
	O−H		0.028	0.100	0.232
	H−H		0.015	0.052	0.103
H	C_1-C_2	0.99	0.261	−0.637	0.098
	C_2-C_3	1.55	0.325	−0.912	0.312
	C_3-C_4	1.13	0.285	−0.737	0.149
	O_1-C_1	1.71	0.395	0.172	0.031
	O_2-C_4	1.68	0.393	0.088	0.054
	C_2-N	1.19	0.316	−0.872	0.090
	$N-C_{1'}$	1.07	0.291	−0.826	0.073
	O−H		0.028	0.099	0.232
	H−H		0.015	0.052	0.104
F	C_1-C_2	1.0	0.261	−0.637	0.098
	C_2-C_3	1.55	0.325	−0.912	0.313
	C_3-C_4	0.13	0.285	−0.737	0.150
	O_1-C_1	1.71	0.395	0.170	0.031
	O_2-C_4	1.68	0.393	0.088	0.054
	C_2-N	1.19	0.316	−0.863	0.091
	$N-C_{1'}$	1.07	0.291	−0.836	0.089
	O−H		0.028	0.100	0.226
	H−H		0.015	0.053	0.104
CF_3	C_1-C_2	1.0	0.261	−0.636	0.098
	C_2-C_3	1.57	0.326	−0.919	0.315
	C_3-C_4	1.12	0.284	−0.732	0.143
	O_1-C_1	1.709	0.395	0.172	0.031
	O_2-C_4	1.69	0.394	0.099	0.055
	C_2-N	1.17	0.314	−0.873	0.084
	$N-C_{1'}$	1.09	0.295	−0.849	0.070
	O−H		0.029	0.101	0.218
	H−H		0.015	0.052	0.107
CN	C_1-C_2	1.0	0.261	−0.637	0.098
	C_2-C_3	1.58	0.327	−0.923	0.316
	C_3-C_4	1.11	0.283	−0.729	0.139
	O_1-C_1	1.71	0.395	0.172	0.032
	O_2-C_4	1.69	0.395	0.105	0.055
	C_2-N	1.16	0.313	−0.871	0.080
	$N-C_{1'}$	1.10	0.297	−0.856	0.072
	O−H		0.029	0.101	0.214
	H−H		0.015	0.052	0.108
NO_2	C_1-C_2	1.0	0.263	−0.647	0.096
	C_2-C_3	1.59	0.328	−0.931	0.314
	C_3-C_4	1.11	0.283	−0.728	0.137
	O_1-C_1	1.71	0.395	0.171	0.035
	O_2-C_4	1.70	0.395	0.111	0.056
	C_2-N	1.16	0.313	−0.884	0.074
	$N-C_{1'}$	1.09	0.298	−0.876	0.070
	O−H		0.026	0.095	0.273
	H−H		0.012	0.049	0.078

and the Laplacians and ellipticities determined with the proaimv program.[23]

According to previously published studies of *N*-phenyl-substituted *p*-quinones,[8] the PM3 calculation predicts strong distortions in the quinone ring which take it out of planarity and pyramidalize both the amine nitrogen atom and the C=O groups.

The geometry of the molecules considered in this study was calculated according to the PM3 method. In this case, for example, for the *p*-NO_2PAN, the $O_1-C_1-C_2-N$ dihedral angle is 11.4°, the $C_2-N-C_{1'}-C_{2'}$ angle is 153.4°, and the $C_2-C_1-C_{8a}-C_8$ angle is 163.8°. For the remaining quinones, the PM3 calculation predicts planar molecules. The C_2-C_3 distance is in agreement with a located double bond. A strong electronic delocalization was detected in the benzene ring fused to the quinone moiety.

Illescas et al.[8] supports the break of planarity of this system with the published geometry of *p*-benzoquinone at −160 °C[24] and of *p*-naphthoquinone.[25] However, the distortion suggested by the experiment is small compared to the distortion shown by *p*-NO_2PAN.

Unlike the previous calculations, the geometry of the *p*-NO_2PAN at Becke3LYP/6-31G(*d*,*p*) level is practically planar in the naphthoquinone moiety with a small distortion of 1.46° in the $O_1-C_1-C_2-N$ angle and of 2.6° in the $C_1-C_2-C_3-C_4$ angle (Table 4). This is in agreement with the experimental data.[24,25] The $C_2-C_3-C_4-C_{4a}$ angle is 0.0° and not 14.7° as predicted by the PM3 calculation. Unlike the other quinones, where the *para*-substituted aromatic ring remains in the plane of the quinone, in *p*-NO_2PAN, the C_2-N bond is rotated, taking the phenyl ring out of the plane. The $C_1-C_2-N-C_{1'}$ angle is 173.7°.

Because the PM3 method is incapable of predicting the *p*-NO_2PAN geometry, the parameters used by this method for calculating quinones are unreliable. We will, therefore, limit our discussion to the results obtained according to the Density Functional Theory.

The nitrogen atom, which binds the quinone and the *para*-substituted phenyl ring, prevents the direct conjugation between the two rings, and interacts with one or the other, determined by the competitive interaction between the two. This is established by the pattern in the $C_{1'}-N-C_2-C_3-C_4-O_2$ bonds which must be carefully analyzed. In the $NO_2 \rightarrow CN \rightarrow CF_3 \rightarrow F \rightarrow H \rightarrow Me \rightarrow OMe$ series (where the electron-donating properties successively increase), we observe substantial elongation of the $C_{1'}-N$ bond, contraction of the $N-C_2$ bond, lengthening of the C_2-C_3 bond, shortening of the C_3-C_4 bond, as well as slight elongation of the C_4-O_2 bond (Table 4). Elongation of the $N-C_1$ bond, also apparent in the same sequence, is compensated by an increase in the angle of the $C_2-N-C_{1'}$ bond, which is 134°, remarkably greater than the expected 120° and which diminishes the steric repulsion between the hydrogen atoms in the C_3-H and $C_{6'}-H$ positions.

Analysis of the natural charges at C_3 and C_1 and the Wiberg bond indexes (Tables 5 and 6) establish that the

(21) Malkin, V. G.; Malkina, O. L.; Eriksson, L. A.; Salahub, D. R. In *Modern Density Functional Theory. A Tool for Chemistry*; Seminario, J. M., Politzer P., Eds.; Elsevier: Amsterdam, 1995.

(22) NBO 4.0. Glendening, E. D.; Badenhoop, J. K.; Reed, A. E.; Carpenter, J. E.; Weinhold, F. Theoretical Chemistry Institute, University of Wisconsin, Madison, WI, 1994. Reed, E. A.; Weinstock, R. B.; Weinhold, F. J. *J. Chem. Phys.* **1985**, *83*, 735−746. Reed, E. A.; Weinhold, F. J. *J. Chem. Phys.* **1985**, *83*, 1736−1740. Reed, E. A.; Curtiss, L. A.; Weinhold, F. *Chem. Rev.* **1988**, *88*, 899−926.

(23) Biegler-Koenig, F. W.; Bader, R. F. W.; Tang, T. H. *J. Comput. Chem.* **1982**, *3*, 317−328.

(24) van Bolhuis, F.; Kiers, C. Th. *Acta Crystallogr. B* **1978**, *34*, 1015−1016.

(25) Gaultier, J.; Hauw, Ch. *Acta Crystallogr.* **1965**, *18*, 179−183.

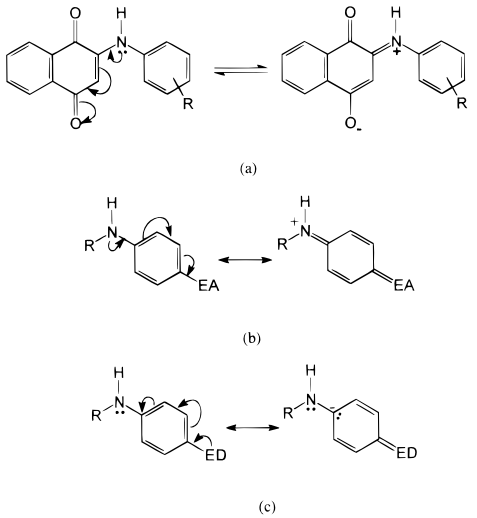

Figure 2. Dominant hybrids of PANs according with the electronic properties of the substituents. (a) Electron delocalization in PANs, (b) effect of the electron-accepting (EA) groups, (c) effect of the electron-donor (ED) groups at the aniline moiety.

geometric behavior is associated with the charge transfer from the *para*-substituted aniline group to the quinone ring, according to the resonant hybrids described in Figure 2a.

In the *p*-NO_2PAN quinone, the nitrogen atom bond to the quinone interacts strongly with the nitro group. The increase in the C_2-N-C_1 angle apparently is insufficient to compensate the H_3-H_6 steric repulsion caused by the shortening of the $N-C_1$ bond. The *p*-nitrophenyl group leaves the plane of the quinone, and the C_2-N rotates. The aromatic ring shows a geometric pattern such as is expected for strong electron-accepting groups. The geometry shows the participation of the resonant hybrids (Figure 2b) which contribute to the delocalization of the electronic density at the nitrogen atom avoiding its displacement in the quinone ring, while the electron-donating groups, resonant hybrids in Figure 2c, dominate, allowing its interaction with the quinone.

We determined the density at bond critical points of the compounds studied according to the Topological Theory of Atoms in Molecules.[26] These densities (Figure 3) agreed with the electronic displacement previously suggested, where the benzene ring of the quinone keeps its aromatic character, and the quinone segment, conjugated with the nitrogen atom, is influenced by the substituent of the aniline-*para*-substituted group.

Figure 3 shows two additional, unexpected bond paths. One of them corresponds to the hydrogen bond between the amine proton and the quinone carbonyl group. The second unexpected critical point corresponds to an interaction line between the attractors of steric origin. These types of interactions have been described by Cioslowski,[27] and the interaction distance ($H_3-H_{6'}$ distance) in the compounds studied here agrees with those reported.[27] Both interactions generate two ring critical points in such a way that the topological relation of Poincarè−Hopf is accomplished. An important difference between these two critical points is that, in the specific case of the critical point defining the hydrogen bridge, the major ellipticity axes are practically parallel to the ring plane. This is considered as an index of electronic delocalization.[27] In the critical point generated by the H−H steric repulsion, however, the axes are perpendicular to the annular plane.

The densities of the critical points studied here strongly depend on the distance between the related attractors, where the density of the critical point diminishes with increasing distance. These critical points are also characterized by a positive Laplacian, which is associated with interactions between closed shell systems, ionic bonds, hydrogen bonds, and van der Waals bonds.[28]

$\nabla^2(\rho)$ is very sensitive to electronic delocalization. This fact is evident in the carbonyl fragments of the compounds studied, since they allow us to effectively differentiate the two quinone carbonyls. The Laplacians of the critical points of the C−O bonds indicate a raised ionic character (Table 6). The C_1-O_1 bond is more electrophilic than the C_4-O_2 bond. The hydrogen bridge, on the other hand, polarizes the C═O group, and the donating aminic nitrogen makes the reduction to nonconjugated carbonyl more susceptible, protecting the C_4-O_2. The Laplacians of critical bond points support the participation of the resonant forms shown in Figure 2a.

Table 7 includes the energies of the frontier molecular orbital, as well as absolute hardness (η), defined as $(E_{LUMO} - E_{HOMO})/2$. For the substituted naphthoquinones, the NBO analysis established that the HOMO orbital corresponds to the lone pairs of one of the heteroatoms. In the *p*-MeOPAN, HOMO orbital corresponds to one of the OMe unshared electronic pairs, the np type, and the HOMO-1 orbital corresponds to the ns type orbital. For the *p*-MePAN, the HOMO corresponds to the unshared pair of the np type of the O_1 atom. In the reference molecule, PAN, the HOMO corresponds to the np type orbital of the oxygen atom, which forms the hydrogen bridge with the NH group. When R is CF_3, the HOMO orbital corresponds to an np orbital associated with one of the group's fluorine atoms. When R is F, the HOMO corresponds to the np orbital of the fluorine atom; for *p*-CNPAN, the HOMO is the np orbital of the nitrogen atom in the nitrile group. When R is NO_2, the HOMO orbital corresponds to an unshared electron pair belonging to one of the oxygen atoms of the nitro group and is of the np type. In all the cases, LUMO corresponds to the Rydberg orbital of the sp type located at C_1. A linear relationship occurs between the HOMO and LUMO orbital energy of these molecules and the experimental σ_p Hammett parameter (eqs 4 and 5).

$$E_{HOMO}(\text{eV}) = -0.2102\sigma_p - 5.1481 \ (n = 7, r = -0.9619) \quad (4)$$

$$E_{LUMO}(\text{eV}) = -0.1388\sigma_p - 2.5321 \ (n = 7, r = -0.9150) \quad (5)$$

Elimination of the molecule with the nitro group increases the correlation. From the conformational point

(26) Bader, R. F. W. *Atoms in Molecules -A Quantum Theory*; Clarendon Press: Oxford, 1990. Bader, R. F. W. *Acc. Chem. Res.* **1985**, *18*, 9−15. Bader, R. F. W. *Chem. Rev.* **1991**, *91*, 893−928. Bader, R. F. W.; Slee, T. S.; Cremer, D.; Kraka, E. *J. Am. Chem. Soc.* **1983**, *105*, 5061−5068.

(27) (a) Cioslowski, J.; Mixon, S. T.; Edwards, W. D. *J. Am. Chem. Soc.* **1991**, *113*, 1083−1085. (b) Cioslowski, J.; Mixon, S. T. *J. Am. Chem. Soc.* **1992**, *114*, 4382−4387.

(28) Cremer, D.; Kraka, E. *Croat. Chem. Acta* **1985**, *57*, 1259−1281.

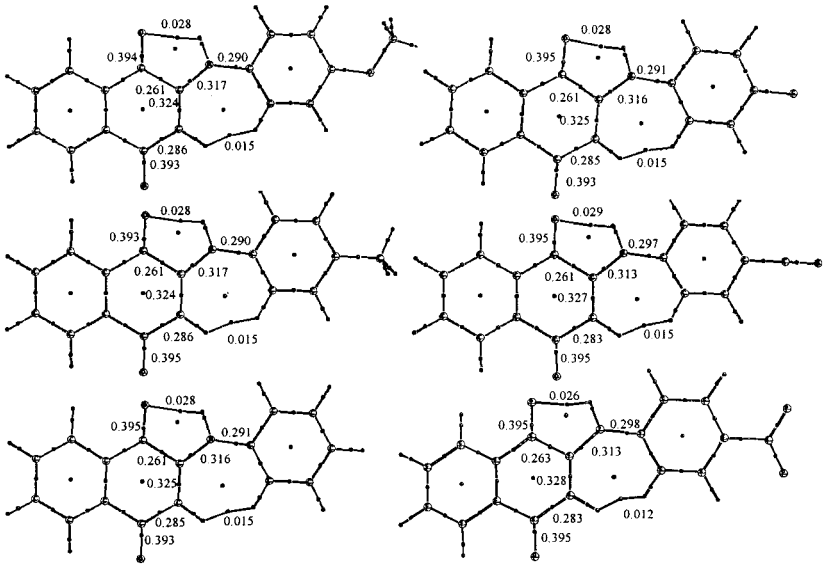

Figure 3. Bond and ring critical points in the density of quinones: *p*-MeOPAN, *p*-MePAN, PAN, *p*-FPAN, *p*-CNPAN, *p*-NO_2-PAN. The values of ρ were obtained into the frame of the topological Theory of Atoms in Molecules.

Table 7. Energy of the Frontier Orbital and Their Neighbors for the Relevant Quinones (energy in hartrees)

R_2	$E_{LUMO} + 1$	E_{LUMO}	E_{HOMO}	$E_{HOMO} - 1$	η	total
OMe	−0.03534	−0.10253	−0.19873	−0.2443	0.0481	−936.07804
Me	−0.03741	−0.10471	−0.20759	−0.24698	−0.05144	−860.87440
H	−0.03911	−0.10647	−0.21268	−0.24899	0.05371	−821.55405
F	−0.04092	−0.10855	−0.21341	−0.25106	−0.05243	−920.78393
CF_3	−0.04710	−0.11461	−0.22553	−0.25745	0.05546	−1158.5897
CN	−0.05791	−0.11941	−0.23131	−0.26166	0.05595	−913.79575
NO_2	−0.10699	−0.13762	−0.25070	−0.28032	0.05654	−1026.05554

of view, the minimum of this molecule is different because it is not a planar molecule. Its conformation thus modifies electronic displacement and the transmission of the substituent's electronic effect. This fact is confirmed by UV−vis experimental data.

The linear relationships (eqs 4 and 5) illustrate that inclusion of the electron-donating group in the aniline ring increases the energy of the border orbitals.

Conclusions

We synthesized 19 2-[(R-phenyl)amine]-1,4-naphthalenediones, nine of which were previously unreported. These compounds are quinone-NH-substituted phenyls (PAN type).

For PAN type molecules, the amine group located between the quinone and the substituted aryl group interferes with direct transmission of the substituent effect on the quinone system. One would thus expect the electronic properties at the quinone radical-anion, generated in the first reduction step, to be distributed solely in the quinone system. However, our analysis of the effect of the substituents on the $E_{1/2}$ potentials for wave I demonstrates that the substituent effect is transmitted through the amine group.

For the compounds studied, we determined the parameters associated with electronic properties ($1/\lambda_{max}$ and $\Delta E_{1/2}$) of the substituent effect which can be assessed by σ_x. Surprisingly, we obtained a linear variation of these electronic properties as a function of σ_x. This variation indicates a direct influence of the donor−acceptor properties of the substituent in the aniline ring on the electronic properties of the quinone ring.

According to Figure 2a, the displacement of the unshared electrons of the aminic nitrogen modifies primarly the electronic density of the C_2-C_3, C_3-C_4, and C_4-O_2 bonds with less effect on the electronic density of the C_1-O_1 bond. These results explain the greater susceptibility of the second reduction wave to the substituent effect (eq 3).

Considering that an electrochemical reduction involves an electron flux from the electrode (cathode) to the substrate (chemical species in solution), the electrons should be gained in the unoccupied molecular orbital of lower energy (LUMO). Hence, when we apply potentials at more negative values, the energies of the electrons increase and eventually they reach sufficiently high energy levels to occupy vacant states over the species in solution. So, the lower the LUMO energy, the easier it will be to achieve the energy level for electrode−solution electron transfer (Figure 4). From the LUMO energy values calculated for the different PANs studied here, we predict that the reduction facility will follow the order: *p*-NO_2 > *p*-CN > *p*-CF_3 > *p*-F > H > *p*-Me > *p*-MeO. The reduction order agrees with the $E_{1/2}$ potentials (Table 2) obtained by cyclic voltammetry for the reduction of PANs in aprotic media. We observed a good linear correlation of the LUMO energy with the corresponding $E_{1/2}$ for Q to $Q^{\bullet-}$ reduction (eq 6). This explains how the $E_{1/2}$ potentials, corresponding to the C_1-O_1 carbonyl reduction, were also subject to the effects of the substituent.

$$E_{1/2}(\text{mV}) = -172.79E_{LUMO}(\text{eV}) - 1707.82 \ (n = 5, r = -0.9855) \quad (6)$$

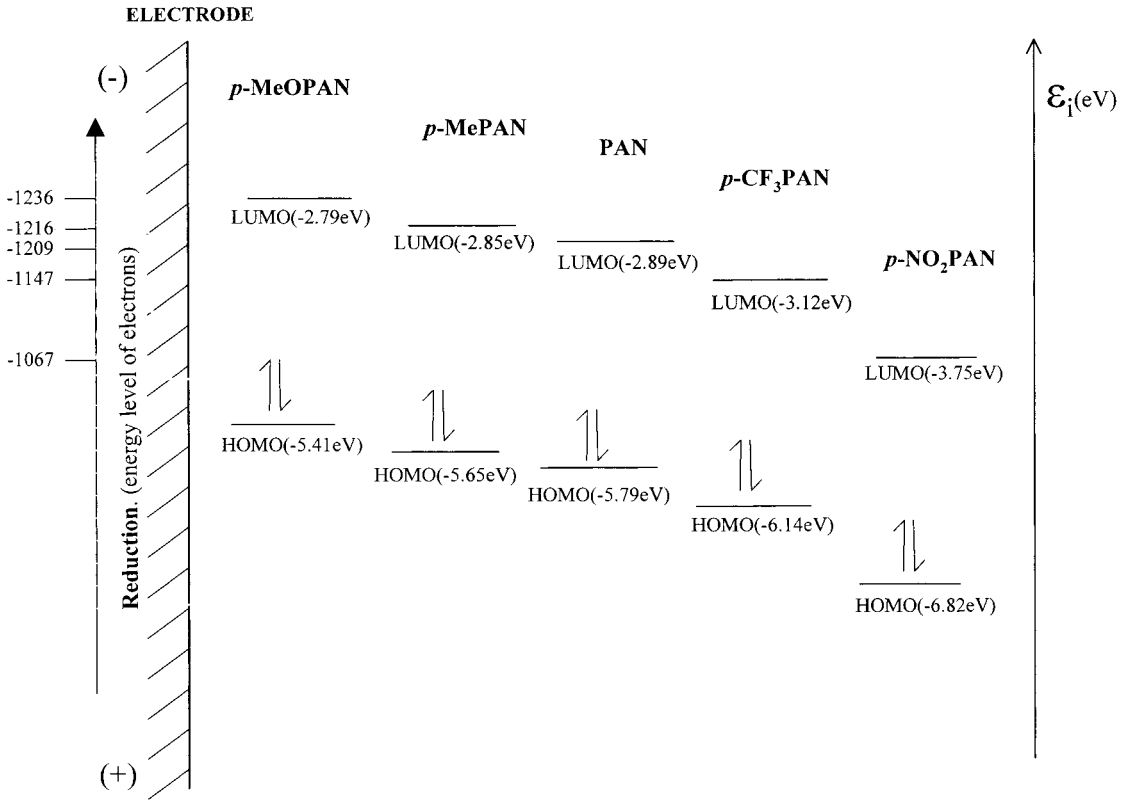

Figure 4. Relationship between energy of HOMO and LUMO molecular orbitals with the donating−acceptor electron properties (oxidation and reduction capability), related to $E_{1/2}$ for first reduction process, in mV.

Experimental Section

Synthesis. NMR spectra were recorded as solutions in $CDCl_3$ at 25 °C on 200 or 300 MHz spectrometers with TMS as reference.

General Procedure for the Preparation of Substituted 2-[(R-phenyl)amine]-1,4-naphthalenediones (PANs). All compounds were prepared by addition of the appropriate aniline to the unsubstituted 1,4-naphthoquinone in ethanol followed by oxidation according to the procedure described by Mohammed et al.,[29] modified by the addition of 0.1 mmol cerous chloride heptahydrate/mol naphthoquinone. $CeCl_3 \cdot 7H_2O$ was powdered and combined with the naphthoquinone before the amine was added. It was reported that the cerium ion catalyzes the addition reaction of *p*-nitroaniline to 1,4-naphthoquinone in the same way as in the reactions of quinolinequinones with aromatic amines.[30] The reaction mixture was left at room-temperature overnight. Crystals of different colors, precipitated from the dark-colored reaction mixtures, were collected by filtration and washed with ethanol until the wash became almost colorless. The residual solids were dried and recrystallized from appropriate solvents.

We only report the spectroscopic characterization of the compounds which have not been previously described (see Table 1).

2-[(3′-Methylphenyl)amine]-1,4-naphthalenedione (*m*-MePAN). Recrystallization from ethanol gave 89% yield; mp 173−175 °C; IR (KBr, cm^{-1}) 3436, 3312, 1670, 1628; UV−vis (EtOH, nm) 272 (21183), 469 (3712); ^{1}H NMR ($CDCl_3$) δ 8.12 (dt, 2H, J = 7.5, J = 1.4 Hz, H_5, H_8) 7.75 (td, 1H, J = 7.5, J = 1.4 Hz, H_7), 7.64 (td, 1H, J = 7.5, J = 1.4 Hz, H_6), 7.54 (sb, 1H, NH); 7.30 (tb,1H, H_5'), 7.10 (sb, 1H, H_2'), 7.02 (db, 2H, J = 7.5 Hz, H_4', H_6'), 6.42 (s, 1H, H_3), 2.4 (s, 3H, CH_3); ^{13}C NMR ($CDCl_3$) δ 183.92 (C_4); 182.06 (C_1), 144.69 (C_2), 139.73 (C_1'), 137.31 (C_2), 134.22 (C_7), 133.22 (C_{10}), 132.27 (C_6), 130.33 (C_9), 129.45 (C_5'), 126.41 (C_4', C_8), 126.11 (C_5), 123.05 (C_2', C_3'), 119.58 (C_6'), 103.30 (C_3), 21.42 (CH_3); CIMS *m*/*z* 263, 248, 234, 220, 218, 206, 191, 158, 130, 105, 91, 77, 57, 43, 41. Anal. Calcd for $C_{17}H_{12}O_2N$: C, 77.56; H, 4.94; N, 5.32. Found: C, 77.18; H, 5.05; N, 5.30.

2-[(3′-Ethylphenyl)amine]-1,4-naphthalenedione (*m*-EtPAN). Recrystallization from ethanol gave 43% yield; mp 119−120 °C; IR (KBr, cm^{-1}) 3304, 3042, 2960, 1672, 1598, 1568, 1484, 1242; UV−vis (EtOH, nm) 272 (54034), 469 (10432); ^{1}H NMR ($CDCl_3$) δ 8.11 (dt, 2H, J = 7.5, J = 1.4 Hz, H_5, H_8), 7.77 (td, J = 7.5, J = 1.4 Hz, H_6), 7.66 (td, J = 7.5, J = 1.4 Hz, H_7), 7.60 (sb, 1H, NH), 7.32 (t, J = 7.5, J = 1.4 Hz, H_5'), 7.11 (sb, 1H, H_6'), 7.10 (d, 1H, J = 7.5 Hz, H_4'), 7.06 (m, 1H, J = 7.5 Hz, H_2'), 6.42 (s, 1H, H_3), 2.67 (q, 2H, J = 7 Hz, CH_2), 1.26 (t, 3H, J = 7 Hz, CH_3); ^{13}C NMR ($CDCl_3$) δ 183.89 (C_4), 182.09 (C_1), 146.12 (C_2), 144.72 (C_1'), 137.37 (C_3'), 134.85 (C_6), 133.24 (C_{10}), 132.26 (C_7), 130.33 (C_9), 129.54 (C_5'), 126.47 (C_8), 126.11 (C_5), 125.22 (C_4'), 121.98 (C_2'), 119.98 (C_6'), 103.30 (C_3), 28.73 (CH_2), 15.40 (CH_3); CIMS *m*/*z* 277, 260, 248, 234, 220, 206, 204, 172, 165, 144, 130, 105, 91, 77, 51, 43, 41. Anal. Calcd for $C_{18}H_{15}O_2N$: C, 77.98; H, 5.41; N, 4.95. Found: C, 77.37; H, 5.37; N, 4.95.

2-[(4′-Ethylphenyl)amine]-1,4-naphthalenedione (*p*-Et-PAN). Recrystallization from ethanol gave 63% yield; mp 150−152 °C; IR (KBr, cm^{-1}) 3444, 3284, 3070, 2962, 1680, 1596, 1588, 1516, 1494, 1348, 1296; UV−vis (EtOH, nm) 272 (27514), 472 (4981); ^{1}H NMR ($CDCl_3$) δ 8.10 (dt, 2H, J = 7.5, J = 1.4 Hz, H_5, H_8), 7.76 (td, 1H, J = 7.5, J = 1.4 Hz, H_7), 7.65 (td, 1H, J = 7.5, J = 1.4 Hz, H_6), 7.52 (sb, 1H, NH), 7.21 (ddq, 4H, J = 7.5, 1.4 Hz, H_2', H_3', H_5', H_6'), 6.37 (s, 1H, H_3), 2.67 (q, 2H, J = 7 Hz, CH_2), 1.25 (t, 3H, J = 7 Hz, CH_3); ^{13}C NMR ($CDCl_3$) δ 183.92 (C_4), 182.11(C_1), 144.99 (C_2), 141.99 (C_1'), 135.00 (C_4'), 134.85 (C_6), 133.27 (C_4'), 133.27 (C_{10}), 132.22 (C_7), 130.35 (C_9), 129.02 (C_2', C_6'), 126.44 (C_5), 126.13 (C_8), 122.94 (C_3'), 122.87 (C_5'),103.11 (C_3), 28.35 (CH_2), 15.54 (CH_3); CIMS *m*/*z* 277, 262, 248, 234, 220, 204, 172,116,105, 77, 43, 41. Anal. Calcd for $C_{18}H_{15}O_2N$: C, 77.97; H, 5.41; N, 5.05. Found: C, 76.87; H, 5.34; N, 4.77.

(29) Mohammed, R. A.; Ayad, M. A.; Chaaban, A. I. *Acta Pharm. Jugoslav* **1976**, *26*, 287.

2-[(4′-*n*-Butylphenyl)amine]-1,4-naphthalenedione (*p*-BuPAN). Recrystallization from ethanol gave 61% yield; mp 112−114 °C; IR (KBr, cm^{-1}) 3284, 2922, 1680, 1590, 1566; UV−vis (EtOH, nm) 272 (30400), 472 (4700); ^1H NMR ($CDCl_3$) δ 8.10 (dt, 2H, J = 7.5, J = 1.4 Hz, H_5, H_8), 7.78 (td, 1H, J = 7.5, J = 1.4 Hz, H_7), 7.65 (td, 1H, J = 7.5, J = 1.4 Hz, H_6), 7.52 (sb,1H, NH), 7.21 (m, 4H, H_2', H_3', H_5', H_6'), 6.37 (s, 1H, H_3), 2.67 (t, 2H, J = 7 Hz, CH_2), 1.60 (q, 2H, J = 7 Hz, CH_2), 1.35 (q, 2H, J = 7 Hz, CH_2), 1.25 (t, 3H, J = 7 Hz, CH_3); ^{13}C NMR ($CDCl_3$) δ 183.75 (C_4), 182.13 (C_1), 145.08 (C_2), 140.71 (C_1'), 134.97 (C_4'), 134.38 (C_6), 133.38 (C_{10}), 132.17 (C_7), 130.46 (C_9), 129.59 (C_2', C_6'), 126.42 (C_5), 126.13 (C_8), 122.75 (C_3', C_5'), 103.11 (C_3), 35.08 (C_7'), 33.47 (C_8'), 22.24 (C_9'), 13.85, (C_{10}); CIMS *m*/*z* 305, 277, 262, 248, 235, 204, 178, 116, 89, 77, 57, 43. Anal. Calcd for $C_{20}H_{19}O_2N$: C, 78.68; H, 6.22; N, 4.59. Found: C, 78.64; H, 6.21; N, 4.48.

2-[(4′-*n*-Hexylphenyl)amine]-1,4-naphthalenedione (*p*-HexPANQ). Recrystallization from ethanol gave 62% yield; mp 100−101 °C; IR (KBr, cm^{-1}) 3450, 3274, 2922, 1690, 1620, 1596, 1568, 1516, 1412; UV−vis (EtOH, nm) 272 (33600), 474 (5500); ^1H NMR ($CDCl_3$) δ 8.00 (dt, J = 7.5 Hz, H_5), 7.72 (td, 1H, H_8), 7.6 (td, J = 7.5, J = 1.4 Hz, H_7), 7.43 (td, J = 7.5, J = 1.4 Hz, H_6), 7.25 (m, 4H, H_2',H_3',H_5',H_6'), 6.41 (s, 1H, H_3), 2.61(t, 2H, J = 7 Hz, CH_2), 1.62 (m, 4H, $2CH_2$), 1.39 (m, 4H, 2CH2), 1.28 (t, 3H, J = 7 Hz, CH_3); CIMS *m*/*z* 333, 262, 248, 235, 178, 116, 105, 89, 77, 43. Anal. Calcd for $C_{22}H_{22}O_2N$: C, 79.27; H, 6.90; N, 4.20. Found: C, 79.02; H, 7.00; N, 4.15.

2-[(3′-Fluorophenyl)amine]-1,4-naphthalenedione (*m*-FPAN). Recrystallization from ethanol gave 53% yield; mp 196−198 °C; IR (KBr, cm^{-1}) 3448, 3316, 3074, 1666, 1640, 1590; UV−vis (EtOH, nm) 276, 456; ^1H NMR ($CDCl_3$) δ 8.1 (dt, 2H, J = 7.5, J = 1.4 Hz, H_5, H_8), 7.77 (td, 1H, J = 7.5, J = 1.4 Hz, H_6), 7.67 (td, 1H, J = 7.5, J = 1.4 Hz, H_7), 7.59 (sb, 1H, NH), 7.40 (td, 1H, J = 7.5, J = 1.4 Hz, H_5'), 7.08 (sb, 1H, H_2'), 7.06 (dt,1H, J = 7.5, J = 1.4 Hz, H_4'), 6.91 (td, 1H, J = 7.5, J = 1.4 Hz, H_6'), 6.46 (s, 1H, H_3); ^{13}C NMR ($CDCl_3$) δ 183.91 (C_4), 181.76 (C_1), 160.00 (C_3'), 144.10 (C_2), 137.65 (C_1'), 134.99 (C_7), 132.50 (C_6), 130.85 (C_5'), 127.06 (C_9), 126.58 (C_8), 126.20 (C_5), 117.88 (C_2') 112.51 (C_6'), 109.78 (C_4'), 104.27 (C_3); CIMS *m*/*z* 267, 266, 239, 238, 222, 211, 185, 183, 162, 149, 129, 105, 83, 69, 57, 55, 43, 41. HRMS for $C_{16}H_{10}O_2NF$ calcd 267.0696, found 267.0702. Anal. Calcd for $C_{16}H_{10}O_2NF$: C, 71.91; H, 3.74; N, 5.24. Found: C, 71.69; H, 3.74; N, 5.24.

2-[(3′-Cyanophenyl)amine]-1,4-naphthalenedione (*m*-CNPAN). Recrystallization from acetonitrile gave 34% yield; mp 296−298 °C; IR (KBr, cm^{-1}) 3306, 3182, 3070, 2226, 1676, 1601, 1575; UV−vis (EtOH, nm) 273, 448; CIMS *m*/*z* 274, 257, 246, 245, 229, 218, 190, 169, 146, 105, 104, 77, 76, 57, 43, 41. HRMS for $C_{16}H_{10}O_2N_2$ calcd 274.0745, found 274.0742. Anal. Calcd for $C_{16}H_{10}O_2N_2$: C, 74.45; H, 3.64; N, 10.21. Found: C, 74.12; H, 4.02; N, 9.83.

2-[(4′-(Trifluoromethyl)phenyl)amine]-1,4-naphthalenedione (*p*-CF_3PAN). Recrystallization from acetonitrile gave 87% yield; mp 185−186 °C; IR (KBr cm^{-1}) 3440, 3234, 3072, 1676, 1634, 1622, 1600, 1574, 1528; UV−vis (EtOH, nm) 271 (35460), 452 (5160) ^1H NMR ($CDCl_3$) δ 8.16 (dt,1H, H_5 or H_8), 8.11 (dt,1H, H_8 or H_5), 7.80 (td, 1H, J = 7.5, J = 1.4 Hz, H_7), 7.69 (td, 1H, J = 7.5, J = 1.4 Hz, H_6), 7.65 (bs, 1H, NH), 7.51 (vbs, 4H, H_2', H_3', H_5', H_6'), 6.43 (s, 1H, H_3); ^{13}C NMR ($CDCl_3$) δ 183.90 (C_4), 181.70 (C_1), 144.25 (C_2), 138.30 (C_1'), 135.07 (C_7), 133.04 (C_{10}), 132.62 (C_9), 132.04 (C_6), 130.37 (C_3'), 126.66 (C_8), 126.31 (C_4', C_5), 125.48 (C_5'), 122.08 (C_2'), 119.24 (C_6'), 104.23 (C_3), 104.06 (C_7'); CIMS *m*/*z* 317, 300, 298, 296; 288, 272, 248, 241, 220, 212, 146, 145, 105, 76, 69, 57, 43, 41. HRMS for $C_{17}H_9O_2NF_3$ calcd 317.0664, found 317.0661. Anal. Calcd for $C_{17}H_9O_2NF_3$: C, 64.15; H, 3.15; N, 4.41. Found: C, 63.87; H, 3.09; N, 4.36.

2-[(3′-Nitrophenyl)amine]-1,4-naphthalenedione (*m*-NO_2PAN). Recrystallization from acetonitrile gave 50% yield; mp 258−260 °C; IR (KBr, cm^{-1}) 3442, 3288, 3214, 3074, 1676, 1604, 1576, 1528, 1352; UV−vis (EtOH, nm) 271 (23600), 447 (4000); ^1H NMR (DMSO) δ 8.25 (bs, 1H, NH), 7.7 to 8.1 (m, 8H, aromatics), 6.3 (s, 1H, H_3); CIMS *m*/*z* 294, 277, 265, 248, 247, 219, 191, 189, 165, 146, 129, 105, 76, 57, 43, 41. HRMS for $C_{16}H_{10}O_4N_2$. Calcd. 294.0655, found 294.0641. Anal. Calcd for $C_{16}H_{10}O_4N_2$: C, 65.30; H, 3.40; N, 9.52. Found: C, 65.01; H, 3.27; N, 9.43.

Electrochemical Procedure. Solvent and Supporting Electrolyte. Acetonitrile (AN) (Aldrich) was dried overnight with $CaCl_2$ (Merck) and purified by distillation on P_2O_5 (Merck) under vacuum.[31] Traces of water in the solvent were eliminated by contact with a molecular sieve 3 Å (Merck) in the absence of light. Tetraethylammonium tetrafluoroborate (Et_4NBF_4) (Fluka) was dried under vacuum at 60 °C.

Electrodes, Apparatus, and Instrumentation. Cyclic voltammetry measurements were carried out in a conventional three-electrode cell. A polished Pt-disk electrode with an area of 3.14 mm^2 was used as a working electrode. Prior to measurements, this electrode was cleaned and polished with 0.05 μm alumina (Buehler), wiped with a tissue, and sonicated in distilled water for 2−4 min. The counter electrode consisted of a piece of platinum wire. The reference electrode was an aqueous saturated calomel electrode (SCE) isolated from the main cell body by a Luggin tube filled with 0.1 M Et_4NBF_4/acetonitrile.

The half-wave potentials were measured at room temperature in acetonitrile solutions using 0.1 M Et_4NBF_4 as the supporting electrolyte. The concentration for the PAN solutions varied from 0.2 mM to 1.0 mM, depending on their solubility in the solvent. Voltammetric curves were recorded using a BAS 100B/W Electrochemical Analyzer of Bioanalytical Systems interfaced with a Gateway 2000 personal computer. Measurements were made over a potential range between 500 to −2000 mV with a sweep rate from 10 to 8000 mV/s. Prior to the experiments, solutions were purged with nitrogen, which was presaturated with the appropriate solvent containing 3 Å sieves. All potentials were determined under the same conditions in order to obtain a consistent data set. To establish a reference system with the experimental conditions of our particular system, the redox potentials reported in this paper refer to the ferrocene/ferrocinium (Fc/Fc^+) pair, as recommended by IUPAC.[32] In this case the potential for the ferrocene/ferrocinium (Fc/Fc^+) redox pair, determined by voltamperometric studies, was 399 mV vs SCE.

Computational Methods. Full geometry optimization (without symmetry constraints) on the complete structures of *p*-MeOPAN, *p*-MePAN, PAN, *p*-FPAN, *p*-CF_3PAN, *p*-CNPAN, *p*-NO_2PAN, and naphthoquinone (NQ) were performed at the PM3 level (Table 3) and according to the DFT at Becke3LYP/6-31G(*d*,*p*) level (Table 4) with the Gaussian 92 Program (G92).[33] The Becke3LYP hybrid functional defines the exchange function as a linear combination of Hartree−Fock, local, and gradient-corrected exchange terms.[34] The exchange function is combined with a local and gradient-corrected correlation function. Substituent groups at the *para*-position in the aniline group were chosen in order to avoid conformational difficulties.

The correlation function used is actually $C*E_CLYP + (1-C)*E_CVWN$, were LYP is the correlation functional of Lee, Yang, and Parr,[35] and includes both local and nonlocal terms. VWN is the Vosko, Wilk, and Nusair 1980 correlation functional fitting the RPA solution to the uniform gas, often referred to

(30) Pratt, Y. T. *J. Org. Chem.* **1962**, *27*, 3905−3910.
(31) Coetzee, J. F.; Cunningham, D. K.; Mc. Guire, D. K.; Padmanabban, A. *Anal. Chem.* **1962**, *34*, 1139−1143.
(32) Gritzner, G. and Küta, J. *Pure Appl. Chem.* **1984**, *4*, 462−466.
(33) G92: Gaussian 92/DFT, Revision G.2. Frisch, M. J.; Trucks, G. W.; Schlegel, H. B.; Gill, P. M. W.; Johnson, B. G.; Wong, M. W.; Foresman, J. B.; Robb, M. A.; Head-Gordon, M.; Replogle, E. S.; Gomperts, R.; Andres, J. L.; Raghavachari, K.; Binkley, J. S.; González, C.; Martin, R. L.; Fox, D. J.; Defrees, D. J.; Baker, J.; Stewart, J. J. P.; Pople, J. A. Gaussian, Inc., Pittsburgh, PA, 1993.
(34) Stephens, P. J.; Devlin, F. J.; Chabalowski, C. F.; Frisch, M. J. *J. Phys. Chem.* **1994**, *98*, 11623−11627. Becke, A. D. *J. Chem. Phys.* **1993**, *98*, 1372−1377, 5648−5652.
(35) Lee, C.; Yang, W.; Parr, R. G. *Phys. Rev.* **1988**, *B37*, 785−789. Miehlich, B.; Savin, A. Stoll, H.; Preuss, H. *Chem. Phys. Lett.* **1989**, *157*, 200−206.

as Local Spin Density (LSD) correlation.[36] VWN is used to provide the excess of local correlation required since LYP contains a local term essentially equivalent to VWN.[34]

The orbital basis set, 6-31G(*d*,*p*), we used adds polarization functions to heavy atoms and hydrogens. Natural Bond Orbital Analyses (NBO) were carried out with version 3.1, which is included in G92.[22] Densities computed at Becke3LYP/6-31G(*d*,*p*) from the G92 output were used with the AIMPAC[23] set of programs to calculate the properties of critical points (cps) in the charge density, density (ρ), Laplacians ($\nabla^2\rho$), and ellipticities (ϵ). Semiempirical PM3[37] full geometrical optimizations of the referred quinones were determined with G92.[33]

Acknowledgment. We are grateful to Dirección General de Servicios de Cómputo Académico, Universidad Nacional Autónoma de México, DGSCA, UNAM, for their computational support, as well as for the generous gift of supercomputer CPU time, and we thank Consejo Nacional de Ciencia y Tecnología (CONACyT) for the financial support given via grants No. 3279P-E9607 and 400313-5-28016E, and Magdalena Kuthy and Anne Sturbaum for careful revision of this manuscript.

JO990186O

(36) Vosko, S. H.; Wilk, L.; Nusair, M. *Can. J. Phys.* **1980**, *58*, 1200−1211.

(37) Stewart, J. J. P. *J. Comput. Chem.* **1989**, *10*, 209−220, 221.